

Consequences of Scapular Anatomy for Reversed Total Shoulder Arthroplasty

Bart Middernacht MD, Pieter-Jan De Roo BSc,
Georges Van Maele MD, PhD, Lieven F. De Wilde MD, PhD

Received: 16 June 2007 / Accepted: 11 February 2008 / Published online: 6 March 2008
© The Association of Bone and Joint Surgeons 2008

Abstract The reverse total shoulder prosthesis provides successful functional outcome in many patients with rotator cuff tear arthropathy. However, scapular notching, a direct consequence of mechanical impingement between the humeral prosthesis and the glenoid, remains a major concern. We presumed a better knowledge of the anatomy of the scapula would enable design or placement modifications to minimize this phenomenon. After establishing a uniform spatial reference system using easy locatable surgical reference points and planes, we analyzed 200 dry bony scapulae and defined the glenoid and infraglenoid anatomy relative to the reference system. The bony rim of the two inferior quadrants of the glenoid forms a semicircle the center of which can be used perioperatively as an easy locatable bony reference point. The infraglenoid tubercle varies in width and length, and can interfere with the humeral part of the reverse prosthesis, creating scapular notching. To avoid notching, we suggest using a convex base plate with a smaller radius than currently used, placing it as low as possible with a 42-mm glenosphere eccentrically assembled to create a posterior offset. If prosthetic overhang cannot be obtained, we suggest removing part of the infraglenoid tubercle.

Introduction

The concept of the reverse prosthesis developed by Grammont and Baulot [16] affords reasonable functional outcome in a rotator-cuff-deficient shoulder. Biomechanical [9, 10] and clinical studies [4, 5, 7, 28, 33, 35, 36] show the reverse prosthesis results in more powerful abduction of the shoulder despite complete loss of rotator cuff function. However, bony wear or remodeling (scapular notching) remains a common radiographic finding at early and late followups [4, 5, 23, 32, 33, 36]. The notch is consistently situated at the inferior pole of the scapular neck (Fig. 1) and is believed to be a source of mechanical failure [4, 5, 27, 32, 36]. Notching occurs in at least 50% of the cases with an increasing size and incidence at longer-term followup [4, 7, 32, 33, 35]. Notching negatively influences not only the mechanical outcome, but also the clinical outcome [32].

Two explanations for notching have been proposed. First, the notch may be secondary to impingement of the medial border of the humeral implant against the inferior rim of the glenoid [4, 7, 26, 35]. Second, mechanical impingement between the polyethylene of the epiphyseal implant and the glenoid during adduction of the arm results in polyethylene wear, causing chronic inflammation of the joint capsule with local osteolysis [27, 35]. Several solutions have been proposed to prevent notching: [4, 15, 26, 27]. Frankle et al. [15] suggested lateralizing the center of rotation outside the scapula, but this creates more torque on the glenosphere and may increase the risk of glenoid loosening in osteoporotic bone [9]. Increasing the inclination (neck-shaft angle) of the humeral component will avoid inferior scapular notching [27] but then may create a superior conflict and enhance prosthetic instability in early abduction [4, 16]. To address the

Each author certifies that he or she has no commercial associations (eg, consultancies, stock ownership, equity interest, patent/licensing arrangements, etc) that might pose a conflict of interest in connection with the submitted article.

Each author certifies that his or her institution has approved the human protocol for this investigation, that all investigations were conducted in conformity with ethical principles of research.

B. Middernacht (✉), P.-J. De Roo, G. Van Maele,
L. F. De Wilde

Department of Orthopaedic Surgery and Traumatology, Ghent University Hospital, De Pintelaan 185, B-9000 Ghent, Belgium
e-mail: bart.middernacht@ugent.be

Fig. 1A–B A (A) radiograph and (B) three-dimensional CT reconstruction show scapular notching.



problem, several companies (Arrow®, Implants Industrie, La Fouillouse, France, and Anatomica® reversed, Zimmer Inc., Warsaw, IN) modified the polyethylene (PE) inlayer to an asymmetric horseshoe shape because in revision surgery retrieved inlayers showed similar wear [27]. An alternative approach is to decrease the prosthetic contact area (Duocentric® Aston Medical France SA, Saint Etienne, France) of the PE but this increases the risk for instability [27]. The benefit from these implant modifications remains to be seen [5]. Some authors attempt to minimize notching by inserting the glenoid component as low as possible [5, 26]. Nyffeler et al. [26] even suggested implanting the metaglene in such a way that the glenosphere has a distal prosthetic overhang to the bone which seems to be the most important factor to reduce the mechanical conflict.

We presumed a better knowledge of the glenoid and scapular neck anatomy could suggest why scapular notching occurs. To identify the cause of notching and ways to better place or design an implant, we searched (1) for an easy locatable and reproducible surgical reference point. Then we analyzed (2) the reproducibility of the midpoint of the circle, formed by the outer rim of the inferior quadrants of the glenoid, as a surgical reference point. We then defined (3) anatomic locations on the glenoid, infraglenoid tubercle and lateral border of the scapula relative to this reference point. With knowledge of these

anatomic locations on the glenoid, we suggest (4) the properties of the best fitting base plate; on the infraglenoid tubercle, we suggest (5) an improved placement of the base plate; and on the lateral border of the scapula, we suggest (6) the ideal placement of the glenosphere on the base plate.

Materials and Methods

We examined 200 dry bone scapulae with and without arthritic changes and identified a potential surgical reference point for establishing a reference frame for quantitatively identifying all anatomic landmarks. There were 100 right and 100 left specimens; the ages were unknown. To ensure we studied scapulae that represent a normal population, we assessed degenerative changes according to the classification of Kerr et al. [21] (O, absent; +, mild; ++, moderate; +++, severe) and we distinguished all glenoids morphologically according to the classification of Walch et al. [38], which describes arthritic erosion in the transverse plane (A1, A2, B1, B2, C) [38] and the classification of Sirveaux et al. [33], which describes erosion in the scapular plane (E0, E1, E2, E3, E4) [33]. We then compared the data with that in the original studies [33, 38]. According to the classification of Kerr et al. [21], we identified 76% mild, 23% moderate, and 1%

severe types of degenerative changes. According to the classification of Walch et al., in the transversal plane of the body, we saw 54.9% A1, 18.3% A2, 25.7% B1, and 1.1% B2 changes, and according to the classification of Sirveaux et al., in the scapular plane of the body, we found 76% E0 and 24% E1 changes.

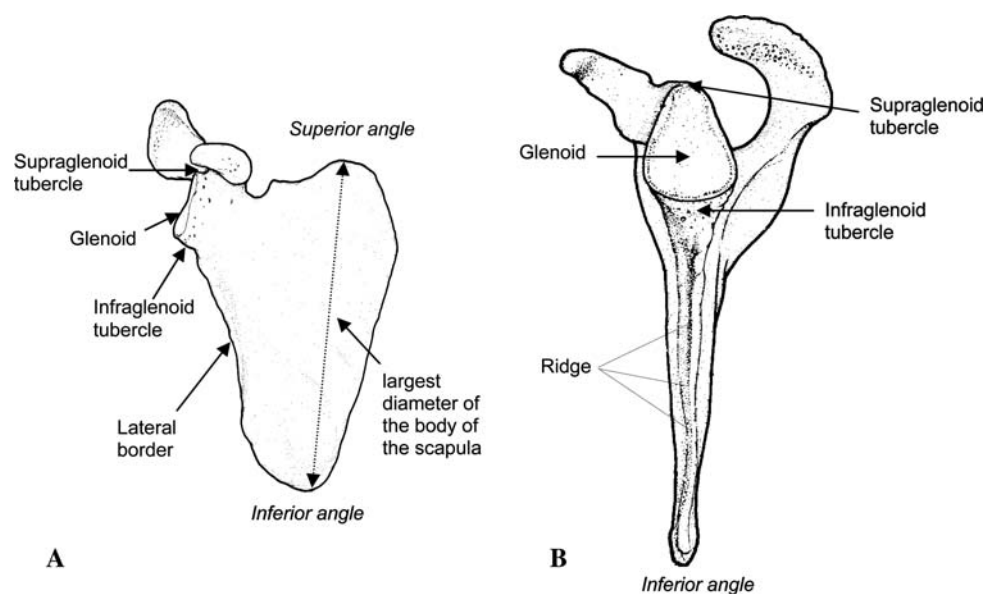
Von Schroeder et al. [37] described a difference in scapular length between men and women but the gender of our cadavers was unknown. However, Mallon et al. [24] suggested differences in measurements between male and female scapulae could be eliminated by normalizing to the length of the cadaver. To ensure a normal population, we therefore normalized all measurements to the largest dimension of the scapula because it has a strong relationship with the length of the cadaver [11, 12, 30]. To ensure similarity of the specimens to that of a normal population, we established Gaussian-like distributions using the Shapiro-Wilk normality test [29]. The largest dimension of the scapular body averaged 153 mm (range, 151.2–155 mm; SD, 13.5 mm; 95% CI). Normalization to the largest dimension of the scapulae confirmed a Gaussian-like distribution of the radius of the circle ($p = 0.28$) and of the superior-inferior distance minus the diameter of the circle ($p = 0.41$).

To establish a reference system for locating landmarks, we first needed a reference plane with an easily established reference point and a reference axis in the plane containing this point. When the reference plane was established, a second plane was created perpendicular to the first and including the reference axis. The third orthogonal plane was established through the reference point. The first investigator (BM) established the reference system twice on five specimens to determine its reproducibility. The intraobserver variability then was determined. We used the

intraclass correlation coefficient in combination with the Wilcoxon signed rank test to assess variability [31]. The intraclass correlation coefficient was 0.982 (range, 0.875–0.998; 95% CI). Once we had an easily reproduced reference system, we could locate anatomic landmarks of the glenoid and scapular neck and define them in three-dimensional space (Fig. 2).

Given the inferior glenoid approximates a semicircle, we defined, by eye (as likely a surgeon would intraoperatively), the best-fitting circle formed by the rim of the two inferior quadrants of each glenoid. We defined the center of this circle as the glenoid midpoint that was located on the bone with a pencil. We also marked the most superior point of the glenoid. A line drawn through these two points using a ruler created the surgical curvilinear line of the glenoid (Fig. 3). Next, we placed a 15-mm-thick custom-made measuring device with a 14.5-mm-radius flat base plate (Fig. 4) onto the glenoid surface. The central hole of this base plate held a Kirschner wire perpendicular to it. We drilled the K wire into the glenoid midpoint to stabilize the base plate. This mimics the perioperative glenoid central hole drilling of the two most commonly used reverse total shoulder prostheses (Delta III; DePuy International Ltd, Leeds, UK, and Aequalis-Reversed; Tornier SA, St-Ismier Cedex, France). The plane of the measuring device in contact with the glenoid rim defined the first reference plane (called the glenoid plane, although we recognize the glenoid fossa is not a planar structure). The superoinferior axis of the coordinate system (Y), was defined by the two contact points between the surgical curvilinear line and the device (Fig. 3). The local origin (0,0,0) of the coordinate system was defined by the intersection of the K wire with the glenoid plane. The three elements needed to create a reference system thus were defined (Fig. 3).

Fig. 2A–B Anatomic landmarks in (A) frontal and (B) lateral views are shown.



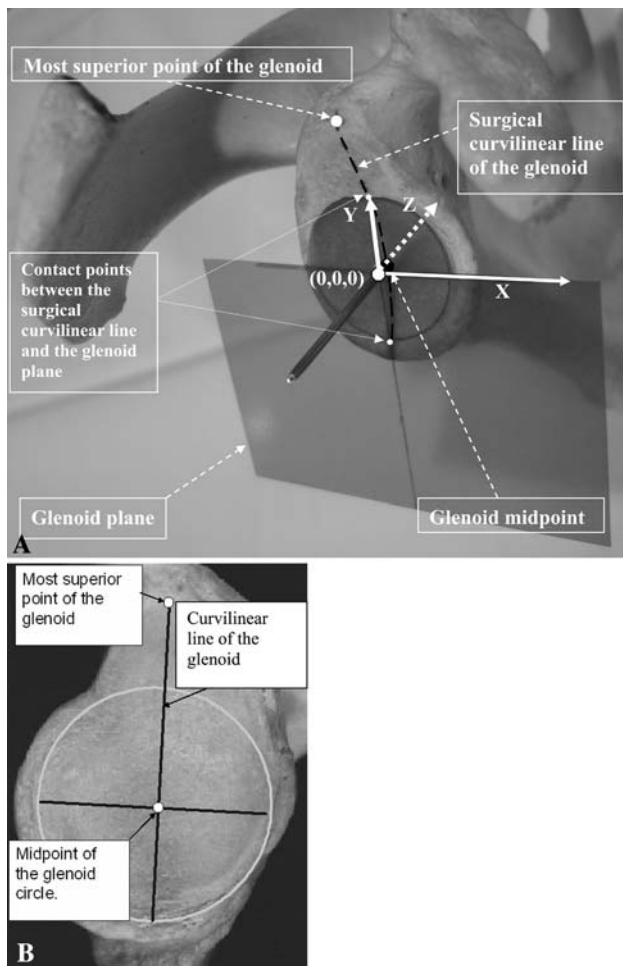


Fig. 3A–B Placement of (A) three-dimensional reference planes and (B) reference points and lines on the glenoid is shown.

We measured anatomic parameters described in a previous study [10] using a ruler: (1) the largest diameter of the body of the scapula, defined by the distance between the superior and inferior angles of the scapula (Fig. 2); (2) the superior-inferior distance of the glenoid (height), defined by the distance between the most superior point of the glenoid fossa and the point where the surgical curvilinear line crosses the infraglenoid border; (3) the anteroposterior distance of the glenoid (width), defined by the length of the axis perpendicular to the surgical curvilinear line drawn through the midpoint of the glenoid; (4) the depth of the glenoid to the device at the midpoint using a depth gauge that could be placed through the central hole of the measuring device (Fig. 4); and (5) location (using the reference frame) and dimensions of the infraglenoid tubercle and axillary border of the scapula; we used the measuring device (Fig. 4) to determine the depth of the axillary border of the scapula relative to the glenoid plane in the mediolateral (scapular) plane at 15, 17, 19, 21, 23, 25, 27, 29, 31, 33, and 35 mm below the glenoid midpoint

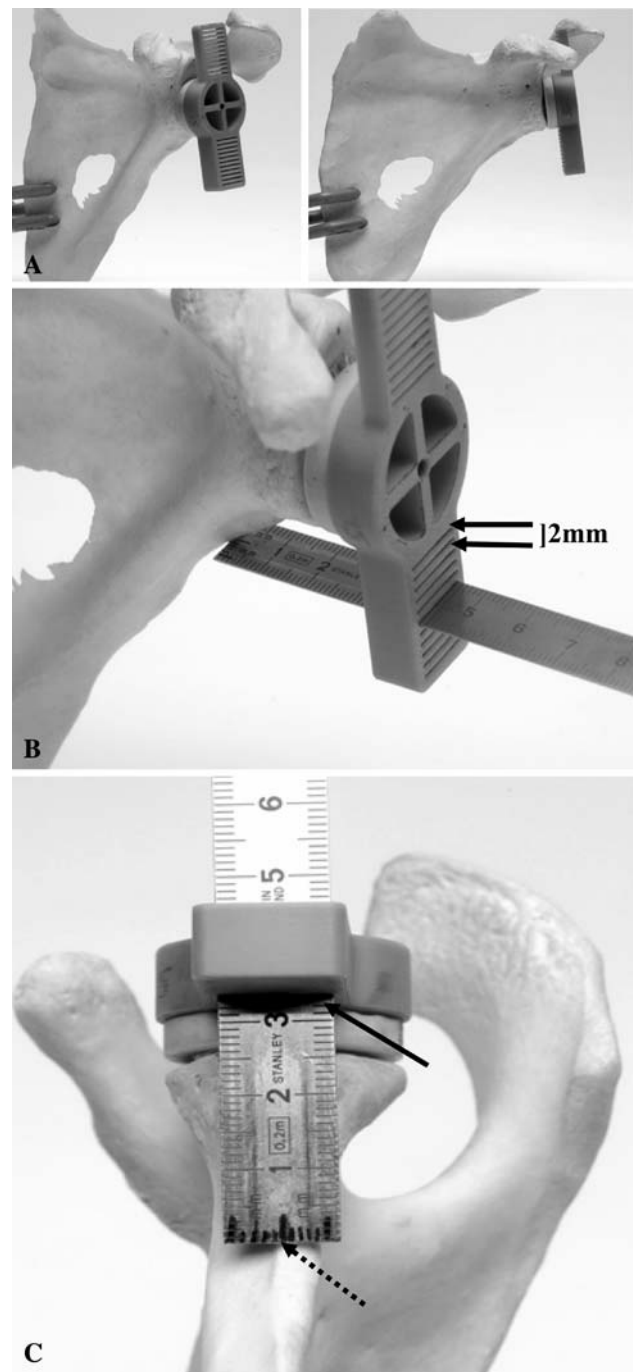


Fig. 4A–C (A) Placement of the measuring device on the glenoid is shown. (B) The ruler is placed through an opening (arrows) to determine the Y distance. (C) Measurement of the X (dotted) and Z (arrows) distances is shown.

in the glenoid plane. A scale at the end of the ruler allowed us to locate the lateral margin in the anteroposterior plane. We defined the anterior position as positive and the posterior position as negative. Linear curve fitting was assessed using a Pearson's correlation coefficient. The measurements of the proximal part of the axillary border

Table 1. Properties of the infraglenoid tubercle

Distance to the glenoid midpoint (mm)	15	17	19	21	23	25
Percentage infraglenoid tubercle present	83.2	74.3	47	20.3	6.9	3.5
Depth to the glenoid plane (mm), mean ± SD	2 ± 4.1	6.4 ± 6	11.7 ± 6.3	16.1 ± 6	19.9 ± 6.2	23.3 ± 6.4

were not possible in 166 scapulae because we could not identify a distinct ridge. However, 27 mm from the glenoid midpoint, all scapulae showed a distinct ridge. We defined the zone that could not be measured accurately as the infraglenoid tubercle (Table 1).

We used trigonometric formulas to calculate: (1) additional adduction obtained by lowering the implant location; lowering the location creates a prosthetic overhang with a certain depth in the scapular plane (d). This extra depth below the prosthesis should allow greater adduction. We used the following equation for a base plate with a radius Rm and a depth d (distance between glenoid plane and lateral scapular border): extra adduction angle = arctg (d/Rm) (Fig. 5); and (2) for approximation of the radius of curvature of the glenoid (Rc) from the known mean depth (D) and mean radius of the glenoid circle (R), the following equation was used: $Rc = (R^2 + D^2)/2D$. (Fig. 7; Appendix 1).

All data of each scapula were recorded in an Excel database (Microsoft, Redmond, WA). We used the SPSS software package (version 12.0; SPSS Inc, Chicago, IL) to analyze the parameters described above.

Correlation was expressed with the Pearson correlation coefficient. The level of significance was set at $\alpha = 0.05$. Normality was evaluated using probability plots (QQ-plot) and the Shapiro-Wilk normality test (low p values indicate the population is nonnormally distributed) [29].

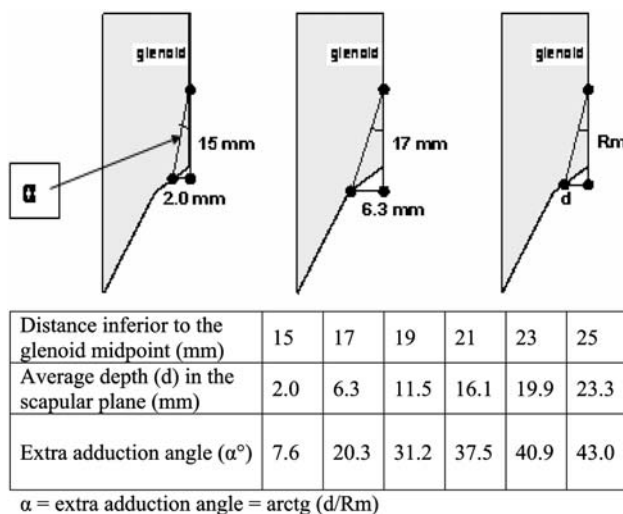


Fig. 5 More prosthetic overhang provides more adduction.

Five different glenoids were analyzed twice by the first investigator to determine the intraobserver variability. To determine these variabilities, the intraclass correlation coefficient was used (ICC), in combination with the Wilcoxon signed ranks test [31].

Results

These data confirmed approximation of the glenoid circle formed by the outer rim of the two inferior quadrants of the glenoid. The mean glenoid width correlated with ($r = 0.80$) the mean height (Fig. 6). The mean glenoid width and height measured 27.9 mm (range, 27.4–28.4 mm; SD, 3.4 mm; 95% CI) and 37.3 mm (range, 36.8–37.8 mm; SD, 3.5 mm; 95% CI), respectively. The mean difference of 9.4 mm (range, 9.1–9.7 mm; SD, 2.2 mm; 95% CI) between these two measurements had a Gaussian distribution ($p = 0.41$). The mean depth of the glenoid to the glenoid plane at the midpoint was 3 mm (range, 2.9–3.2 mm; SD, 0.8 mm; 95% CI). The mean radius of curvature of the glenoid (Rc), calculated from the known mean depth (D) and mean radius of the glenoid circle (R), was 33.6 mm (range, 31.4–36 mm; 95% CI) (Fig. 7).

For a 36-mm metaglène, lowering the insertion place 2 mm, for instance, creates a greater prosthetic overhang with an average added depth in the scapular plane (d) of 4.3 mm, and an artificial extra adduction angle of 13° can be gained (Fig. 5).

In the scapular view of the body, the measured axillary border formed a straight line as suggested by the linear regression line (correlation coefficient, 0.868) and had an angulation of 54° (SD 6°) to the glenoid plane (Fig. 8). The

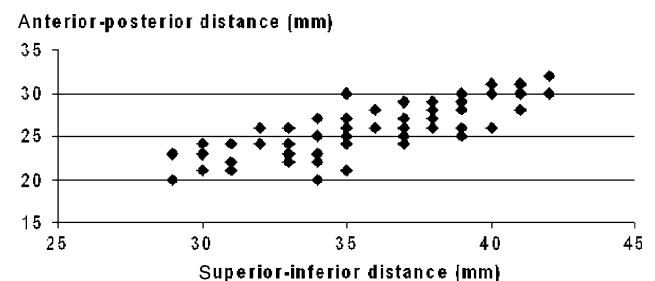


Fig. 6 The relationship between the anterior-posterior and the superior-inferior distance prove the existence of the glenoid circle.

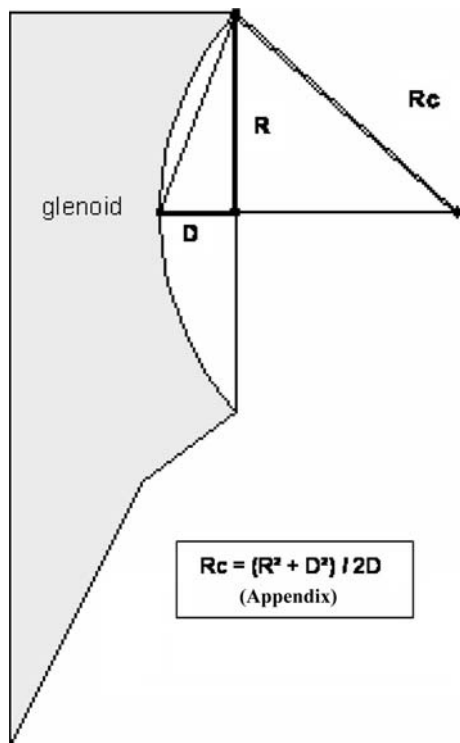
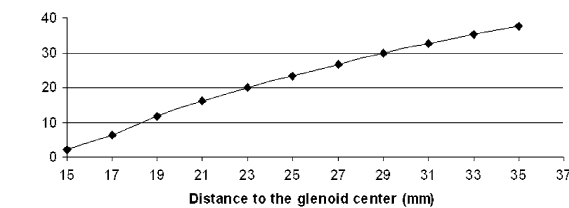


Fig. 7 Calculation of the radius of curvature of the glenoid using $R_c = (R^2 + D^2)/2D$ is shown.

Average depth (mm; 95% CI) of the lateral border of the scapula relative to the glenoid axis.



15	17	19	21	23	25	27	29	31	33	35
2	6.4	11.7	16.1	19.9	23.3	26.6	29.9	32.6	35.2	37.7
±0.6	±0.8	±0.9	±0.9	±0.9	±0.9	±0.9	±0.9	±0.9	±0.9	±1.0

Fig. 8 The position of the axillary border of the scapula in the scapular plane relative to the glenoid is shown.

regression coefficient of this line averaged 1.43 (range, 1.39–1.47; SD, 0.3; 95% CI). We extrapolated this line into the infraglenoid tubercle. After flat reaming the glenoid with placement of the base plate as distally as possible, this tubercle forms a bone mass just inferior to the assembled glenosphere and with a thickness of 4 mm or 1 mm when using the 36-mm or the 42-mm designs, respectively, on the ridge (Table 2).

Viewing the body directly facing the glenoid, the anterior part of the ridge of the axillary border formed a straight line parallel to the surgical curvilinear line, whereas the posterior wall was more oblique, converging toward the inferior angle of the scapula (Fig. 9). In this plane, the

Table 2. Calculated thickness of the infraglenoid tubercle on the scapular ridge

Prosthesis size (mm)	Distance to glenoid midpoint (mm)	Depth to scapular ridge (mm) (calculated*)	Depth to infraglenoid tubercle** (mm)	Thickness of infraglenoid tubercle on the crista (mm)
36	18	13.3	9.1	4.2
38	19	14.7	11.7	3
40	20	16.2	13.9	2.2
42	21	17.6	16.1	1.5

* Depth calculated using the mathematical formula describing the margo lateralis in the scapular plane relative to the glenoid plane: $y = 1.43 \times -12.45$; ** depth measured relative to the glenoid plane.

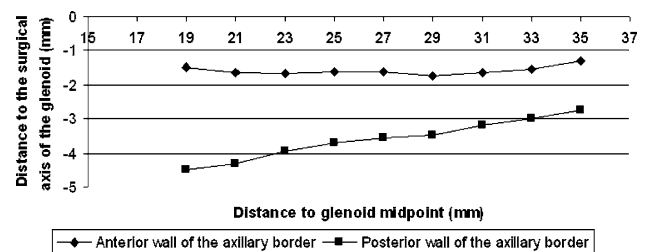


Fig. 9 The posterior position of the axillary border of the scapula in the glenoid plane relative to the surgical curvilinear line is shown.

lateral border of the scapula had a mean posterior offset relative to the surgical curvilinear line of 1.7 mm (range, 1.63–1.77 mm; 95% CI).

Discussion

The reverse total shoulder prosthesis, originally designed by Grammont and Baulot [16], is becoming more popular in shoulder replacement arthroplasty [4, 6, 9, 14, 15, 18, 27, 33]. However, mechanical contact between the bony cortex of the scapula and the humeral prosthetic epiphysis may limit range of motion [27] and cause development of scapular notching, [5, 27] which is known to compromise the clinical outcome and increase the risk of glenoid loosening [5, 18, 26, 32, 33]. For these reasons, some shoulder surgeons advise using the deltopectoral approach rather than the anterosuperior approach [33] and implanting the glenosphere in some degree of varus [16, 19]. However, the mechanical contact also exists in the transverse plane of the body, thereby limiting the range of external and internal rotation and sometimes resulting in mechanical prosthetic failure [8].

We believe the main limitation of our study is that all the measurements were performed by one observer, therefore only intraobserver reliability and no interobserver reliability could be determined to evaluate the reproducibility of the reference system. We believe the

interobserver variability would be small but this cannot be confirmed.

A thorough knowledge of the anatomy of the glenoid, the infraglenoid tubercle, and the lateral border of the scapula should help explain the anatomic cause of scapular notching. We found the midpoint of the best fitting inferior glenoid circle an easily locatable surgical reference point and defined the anatomy of the glenoid and scapular neck referring to this reference point. A better knowledge of the anatomy can be used to adjust the design and placement of the reverse prosthesis and minimize scapular notching. Clinical studies can confirm or refute our findings.

The distribution of osteoarthritic changes in the bony scapulae was similar to that described by Kerr et al. [21] and Walch et al. [38] for general grading and transverse classification, respectively, as described in their original studies (Table 3). Numerous anatomic parameters behave in a Gaussian-like manner after being normalized for gender, which led us to believe the studied scapulae are representative for a normal adult population [33, 37].

Our data suggest the bony surface of the glenoid is composed of two parts: a circular inferior glenoid and a noncircular cranial extension, of which the supraglenoid tubercle is the most superior and lateral point. This probably can be explained by the development of the bony glenoid where two centers appear during growth. One appears during the 10th year and contributes to the formation of the base of the coracoid and the upper end of the glenoid. It fuses to the scapula during the 15th year. The second one is a horseshoe-shaped ossific center, appearing around puberty, which contributes to the formation of the lower portion of the glenoid [10]. Because the circle always can be defined accurately, the actual circular shape of the prosthetic glenoid base plate can be accepted. However, if the center of this circle is taken as a point of reference for implantation and the base plate is placed onto the glenoid midpoint, 57% will have prosthetic overhang. Therefore, we suggest a smaller base plate. We calculated the mean radius of the glenoid circle to be 14 mm (SD, 1.7 mm). To minimize the loss of bony contact with a smaller base plate we advise using a convex reamer instead

of a flat reamer. This would enlarge the contact area of the base plate for the same diameter and would minimize bony resection of the glenoid so the strength of the subchondral plate of the glenoid is minimally weakened. The mean curvature for such a reamer was 34 mm (Fig. 7), which is consistent with reported curvature [25]. Theoretically, a convex base plate improves prosthetic glenoid fixation, as has been documented in anatomic shoulder prostheses [2, 3, 22, 34]. Another implication of this practice is the size of the glenosphere with its center of rotation placed at the glenoid subchondral plate, identical to the original design by Grammont and Baulot, can be smaller than half a sphere without compromising the prosthetic overhang (Fig. 10). This decrease in prosthetic bulkiness eases surgery but lowers the contact area between the prosthetic elements.

The current practice to minimize notching is to insert the base plate as low as possible [5, 26]. Nyffeler et al. [26] reported this creates a prosthetic overhang if the glenosphere is assembled. This seems the most important factor to reduce the mechanical contact. For a 36-mm design, we calculated that 2-mm of lowering, for example, with the associated extra prosthetic overhang creates an extra adduction of approximately 13° (Fig. 5).

This prosthetic overhang could not always be created by placing the base plate as distally as possible because of the presence of an infraglenoid tubercle. For a 36-mm glenosphere assembled to a base plate positioned as distally as possible, a prosthetic overhang could not be created in 75% (150 scapulae) and for a 42-mm design in 27% (55 scapulae). Therefore, we recommend using a 42-mm design. This is in contrast with the findings of Lévine et al. [23], who suggested a greater risk of scapular notching with a larger diameter humeral cup and glenosphere. Their suggestion, however, did not include prosthetic overhang, which we believe important.

In cases where prosthetic overhang cannot be created, we suggest removing part of the infraglenoid tubercle

Table 3. Comparison of distribution of glenoid osteoarthritic changes

Classification	Absent	Mild	Moderate or Severe		
Kerr et al. [21]	21%	51%	28%		
Current study	0%	76%	24%		
	Type A1	Type A2	Type B1	Type B2	Type C
Walch et al. [38]	43%	16%	17%	15%	9%
Current study	55%	18%	26%	1%	0%

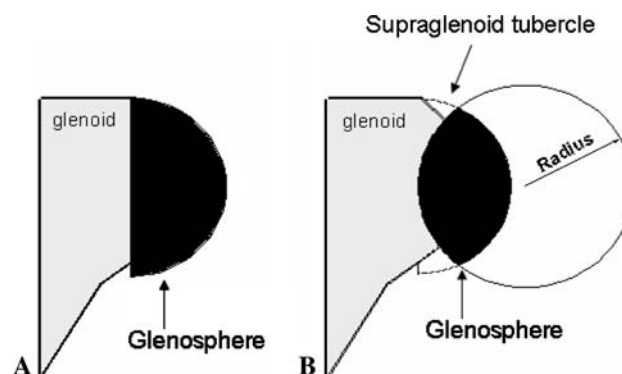
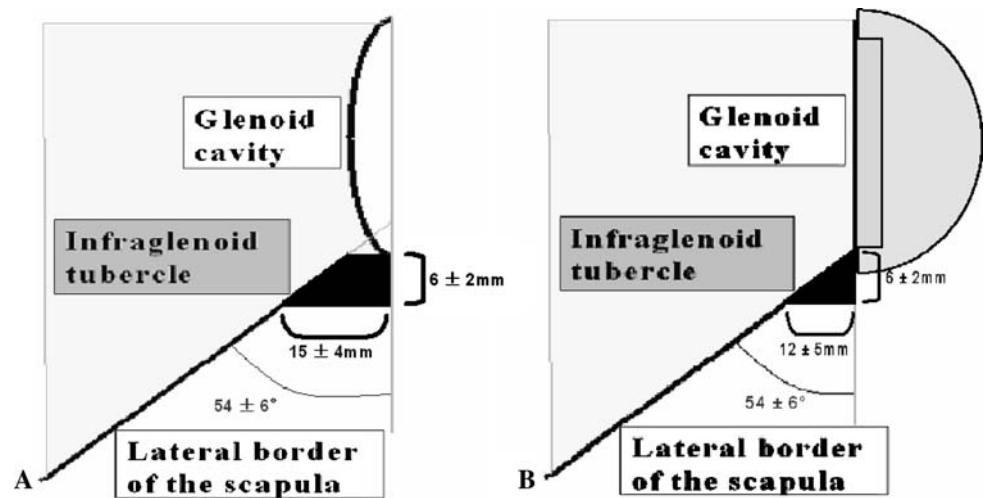


Fig. 10A–B The differences in glenosphere placement between a (A) flat base plate and a (B) convex base plate are shown. Both have the same center of rotation.

Fig. 11A–B Properties of the infraglenoid tubercle and the lateral border of the scapula in (A) an anatomic setting and in (B) prosthetic setting are shown.



(Fig. 11) on the inferior bony scapular pillar as described below without weakening this pillar since it is the most important supporting structure of the glenoid. The pillars are outlined by three cortices and orientated to the circle formed by the rim of the inferior quadrants of the glenoid. The inferior pillar is directed inferiorly near the lateral border of the scapula [1, 20]. When the proximal portion of the ridge (the most lateral point of the scapular pillar) was imaginarily extended superiorly to the infraglenoid tubercle, our measurements indicated that after flat reaming the glenoid and placing the base plate as distally as possible, 4 mm or 1 mm of the tubercle could be removed just inferior to the glenosphere when using the 36-mm or the 42-mm design, respectively (Table 2) without removing or weakening the scapular pillar. This resection may include the entire infraglenoid tubercle in the glenoid plane of the body. Part of the origin of the triceps brachii muscle will be lost by this resection, but this will not interfere with shoulder stability [13, 17]. We advise preservation of the detached inferior capsule at the tendinous origin of the long head of the triceps tendon to make this resection a safe surgical maneuver; the axillary nerve is protected by doing so.

Because of the posterior offset of the lateral border of the scapula in the glenoid plane, one can expect that mainly passive external rotation in adduction will be limited by mechanical conflict between this lateral border and the humeral prosthesis. To solve this problem, the surgeon can either optimize the relationship between the humeral and glenoid placement in the transverse plane of the scapular body or introduce a posterior offset to the glenoid of the reverse prosthesis by eccentrically assembling the glenosphere to the glenoid base plate.

Acknowledgments We acknowledge the support of Rene Verdonk, MD, PhD.

Appendix 1

$$A^2 = R^2 + D^2 \qquad \text{Tg}(\alpha) = R / D$$

$$A = \sqrt{R^2 + D^2} \qquad \alpha = \text{arctg}(R/D)$$

$$\cos(\alpha) = (A/2) / Rc$$

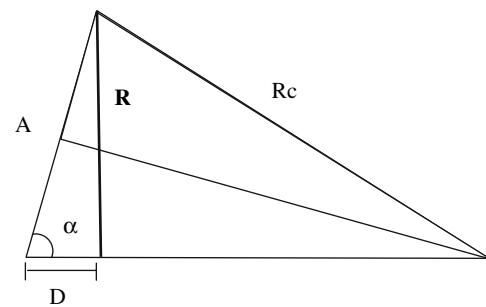
$$\cos(\alpha) = A / 2 Rc$$

$$Rc = A / 2 \cdot \cos(\alpha)$$

$$Rc = A / 2 \cdot (D/A)$$

$$Rc = A^2 / 2D$$

$$Rc = (R^2 + D^2) / 2D$$



References

1. Anetzberger H, Putz R. The scapula: principles of construction and stress. *Acta Anat.* 1996;156:70–80.
2. Anglin C, Wyss UP, Nyffeler RW, Gerber C. Loosening performance of cemented glenoid prosthesis design pairs. *Clin Biomech (Bristol, Avon).* 2001;16:144–150.
3. Anglin C, Wyss UP, Pichora DR. Mechanical testing of shoulder prostheses and recommendations for glenoid design. *J Shoulder Elbow Surg.* 2000;9:323–331.
4. Boileau P, Watkinson DJ, Hatzidakis AM, Balg F. Grammont reverse prosthesis: design, rationale, and biomechanics. *J Shoulder Elbow Surg.* 2005;14(1 suppl S):147S–161S.
5. Boileau P, Watkinson D, Hatzidakis AM, Hovorka I. Neer Award 2005: The Grammont reverse shoulder prosthesis: results in cuff tear arthritis, fracture sequelae, and revision arthroplasty. *J Shoulder Elbow Surg.* 2006;15:527–540.
6. Boulahia A, Edwards TB, Walch G, Baratta RV. Early results of a reverse design prosthesis in the treatment of arthritis of the

- shoulder in elderly patients with a large rotator cuff tear. *Orthopedics*. 2002;25:129–133.
7. Delloye C, Joris D, Colette A, Eudier A, Dubuc JE. Complications mécaniques de la prothèse inversée de l'épaule. *Rev Chir Orthop Reparatrice Appar Mot*. 2002;88:410–414.
 8. De Wilde L, Walch G. Humeral prosthetic failure of reversed total shoulder arthroplasty: a report of three cases. *J Shoulder Elbow Surg*. 2006;15:260–264.
 9. De Wilde LF, Audenaert EA, Berghs BM. Shoulder prostheses treating cuff tear arthropathy: a comparative biomechanical study. *J Orthop Res*. 2004;22:1222–1230.
 10. De Wilde LF, Berghs BM, Audenaert E, Sys G, Van Maele GO, Barbaix E. About the variability of the shape of the glenoid cavity. *Surg Radiol Anat*. 2004;26:54–59.
 11. Dilmén G, Turhan NO, Toppare MF, Seckin N, Ozturk M, Goksin E. Scapula length measurement for assessment of fetal growth and development. *Ultrasound Med Biol*. 1995;21:139–142.
 12. Di Vella G, Campobasso CP, Dragone M, Introna F Jr. Skeletal sex determination by scapular measurements. *Boll Soc Ital Biol Sper*. 1994;70:299–305.
 13. Eiserloh H, Drez D Jr, Guanche CA. The long head of the triceps: a detailed analysis of its capsular origin. *J Shoulder Elbow Surg*. 2000;9:332–335.
 14. Favard L, Lautmann S, Sirveaux F. Hemi arthroplasty versus reverse arthroplasty in the treatment of osteoarthritis with massive rotator cuff tear. In: Walch G, Boileau P, Mole D, eds. *2000 Shoulder Prostheses: Two to Ten Year Follow-up*. Montpellier, France: Sauramps Medical; 2001:261–268.
 15. Frankle M, Levy JC, Pupello D, Siegal S, Saleem A, Mighell M, Vasey M. The reverse shoulder prosthesis for glenohumeral arthritis associated with severe rotator cuff deficiency: a minimum two-year follow-up study of sixty patients: surgical technique. *J Bone Joint Surg Am*. 2006;88(suppl 1 pt 2):178–190.
 16. Grammont PM, Baulot E. Delta shoulder prosthesis for rotator cuff rupture. *Orthopedics*. 1993;16:65–68.
 17. Gray H. *Anatomy of the Human Body*, 20th ed. Revised and reedited by Lewis WH. Philadelphia, PA: Lea & Febiger; 1918. Bartleby.com, 2000. Available at: <http://www.bartleby.com/107/>; accessed 20 May 2007.
 18. Guery J, Favard L, Sirveaux F, Oudet D, Mole D, Walch G. Reverse total shoulder arthroplasty: survivorship analysis of eighty replacements followed for five to ten years. *J Bone Joint Surg Am*. 2006;88:1742–1747.
 19. Gutiérrez S, Greiwe RM, Frankle MA, Siegal S, Lee WE 3rd. Biomechanical comparison of component position and hardware failure in the reverse shoulder prosthesis. *J Shoulder Elbow Surg*. 2007;16(3 suppl):S9–S12.
 20. Karelse A, Kegels L, De Wilde L. The pillars of the scapula. *Clin Anat*. 2007;20:392–399.
 21. Kerr R, Resnick D, Pineda C, Haghighi P. Osteoarthritis of the glenohumeral joint: a radiologic–pathologic study. *AJR Am J Roentgenol*. 1985;144:967–972.
 22. Lacaze F, Kempf JK, Bonnomet F, Boutemy P, Colin F. Primary fixation of glenoid implants: an in vitro study. In: Walch G, Boileau P, eds. *Shoulder Arthroplasty*. Berlin, Germany: Springer; 1999:141–146.
 23. Lévine CH, Boileau P, Favard L, Garaud P, Molé D, Sirveaux F, Walch G. Scapular notching in reverse shoulder arthroplasty. In: Walch G, Boileau P, Mole D, Favard L, Lévine C, Sirveaux F, eds. *Reverse Shoulder Arthroplasty*. Montpellier, France: Sauramps Medical; 2006:353–372.
 24. Mallon WJ, Brown HR, Volgler JB 3rd, Martinez S. Radiographic and geometric anatomy of the scapula. *Clin Orthop Relat Res*. 1992;277:142–154.
 25. McPherson EJ, Friedman RJ, An YH, Chokesi R, Dooley RL. Anthropometric study of normal glenohumeral relationships. *J Shoulder Elbow Surg*. 1997;6:105–112.
 26. Nyffeler RW, Werner CM, Gerber C. Biomechanical relevance of glenoid component positioning in the reverse Delta III total shoulder prosthesis. *J Shoulder Elbow Surg*. 2005;14:524–528.
 27. Nyffeler RW, Werner CML, Simmen BR, Gerber C. Analysis of a retrieved Delta III total shoulder prosthesis. *J Bone Joint Surg Br*. 2004;86:1187–1191.
 28. Rittmeister M, Kerschbaumer F. Grammont reverse total shoulder arthroplasty in patients with rheumatoid arthritis and nonreconstructible rotator cuff lesions. *J Shoulder Elbow Surg*. 2001;10:17–22.
 29. Shapiro SS, Wilk MB. An analysis of variance test for normality (complete samples). *Biometrika*. 1965;52:591–611.
 30. Sherer DM, Plessinger MA, Allen TA. Fetal scapular length in the ultrasonographic assessment of gestational age. *J Ultrasound Med*. 1994;13:523–528.
 31. Shrout PE, Fleiss JL. Intraclass correlations: uses in assessing rater reliability. *Psychological Bulletin*. 1979;86:420–428.
 32. Simovitch RW, Zumstein MA, Lohri E, Helmy N, Gerber C. Predictors of scapular notching in patients managed with the Delta III reverse total shoulder replacement. *J Bone Joint Surg Am*. 2007;89:588–600.
 33. Sirveaux F, Favard L, Oudet D, Huquet D, Walch G, Molé D. Grammont inverted total shoulder arthroplasty in the treatment of glenohumeral osteoarthritis with massive rupture of the cuff: results of a multicentre study of 80 shoulders. *J Bone Joint Surg Br*. 2004;86:388–395.
 34. Szabo I, Buscayret F, Edwards TB, Nemoz C, Boileau P, Walch G. Radiographic comparison of flat-back and convex-back glenoid components in total shoulder arthroplasty. *J Shoulder Elbow Surg*. 2005;14:636–642.
 35. Valenti P, Boutens D, Nerot C. Delta 3 reversed prosthesis for arthritis with massive rotator cuff tear: long term results (> 5 years). In: Walch G, Boileau P, Molé D, eds. *2000 Shoulder Prostheses: Two to Ten Year Follow-up*. Montpellier, France: Sauramps Medical; 2001:253–259.
 36. Vanhove B, Beugnies A. Grammont's reverse shoulder prosthesis for rotator cuff arthropathy: a retrospective study of 32 cases. *Acta Orthop Belg*. 2004;70:219–225.
 37. von Schroeder HP, Kuiper SD, Botte MJ. Osseous anatomy of the scapula. *Clin Orthop Relat Res*. 2001;383:131–139.
 38. Walch G, Badet R, Boulahia A, Houry A. Morphologic study of the glenoid in primary glenohumeral osteoarthritis. *J Arthroplasty*. 1999;14:756–760.